Design, modeling, synthesis and biological activity evaluation of camptothecin-linked platinum anticancer agents

ARTICLE *in* EUROPEAN JOURNAL OF MEDICINAL CHEMISTRY · MARCH 2013

Impact Factor: 3.45 · DOI: 10.1016/j.ejmech.2013.02.022 · Source: PubMed

10 AUTHORS, INCLUDING:

Loana Musso
University of Milan
33 PUBLICATIONS **169** CITATIONS

SEE PROFILE

Roberto Artali
Scientia Advice di Roberto Artali
58 PUBLICATIONS **453** CITATIONS

SEE PROFILE

European Journal of Medicinal Chemistry 63 (2013) 387–400

Contents lists available at SciVerse ScienceDirect

European Journal of Medicinal Chemistry

journal homepage: http://www.elsevier.com/locate/ejmech

Original article

Design, modeling, synthesis and biological activity evaluation of camptothecin-linked platinum anticancer agents

Raffaella Cincinelli [a], Loana Musso [a], Sabrina Dallavalle [a,*], Roberto Artali [b], Stella Tinelli [c], Donato Colangelo [d], Franco Zunino [c], Michelandrea De Cesare [c], Giovanni Luca Beretta [c], Nadia Zaffaroni [c]

[a] Department of Food, Environmental and Nutritional Sciences, Division of Chemistry and Molecular Biology, Università di Milano, Via Celoria 2, 20133 Milano, Italy
[b] Scientia Advice, Via Galileo Ferraris 28, 20851 Lissone (MB), Italy
[c] Molecular Pharmacology Unit, Department of Experimental Oncology and Molecular Medicine, Fondazione IRCSS Istituto Nazionale Tumori, Via Amadeo 42, 20133 Milan, Italy
[d] Università del Piemonte Orientale, Via Solaroli 17, 28100 Novara, Italy

ARTICLE INFO

Article history:
Received 4 December 2012
Received in revised form
14 February 2013
Accepted 19 February 2013
Available online 1 March 2013

Keywords:
Antitumor compounds
Docking
Camptothecin
Diaminedichloro-platinum (II)

ABSTRACT

The design, modeling, synthesis and biological activity evaluation of two hybrid agents formed by 7-oxyiminomethylcamptothecin derivatives and diaminedichloro-platinum (II) complex are reported. The compounds showed growth inhibitory activity against a panel of human tumor cell lines, including sublines resistant to topotecan and platinum compounds. The derivatives were active in all the tested cell lines, and compound **1b**, the most active one, was able to overcome cisplatin resistance in the osteosarcoma U2OS/Pt cell line. Platinum-containing camptothecins produced platinum-DNA adducts and topoisomerase I-mediated DNA damage with cleavage pattern and persistence similar to SN38, the active principle of irinotecan. Compound **1b** exhibited an appreciable antitumor activity *in vivo* against human H460 tumor xenograft, comparable to that of irinotecan at lower well-tolerated dose levels and superior to cisplatin. The results support the interpretation that the diaminedichloro-platinum (II) complex conjugated via an oxyiminomethyl linker at the 7-position of the camptothecin resulted in a new class of effective antitumor compounds.

1. Introduction

The antitumor activity of cis-diaminedichloro-platinum (II) (cisplatin or cDDP, Chart 1) was first reported by Rosenberg et al. in 1969 [1]. The success of cisplatin paved the way for the second and third-generation platinum(II) drugs, carboplatin and oxaliplatin (Chart 1). Presently, platinum-based coordination complexes are among the most widely used antitumor agents in the clinic [2]. The effectiveness of cisplatin lies in its ability to covalently bind DNA, leading to important changes in the helical structure. In spite of the efficacy of platinum-based treatment regimens, long-term cure is difficult to obtain. The major drawbacks include a) severe and sometimes life-threatening toxic side effects; b) activation of drug resistance mechanisms by tumor cells; c) inadequate intratumor concentration of the drug and tumor microenvironmental interactions; d) relatively poor pharmacokinetic profiles and e) increased DNA repair capacity [3–5].

Recently, major effort has been made to develop new platinum complexes. Often, the strategies were aimed to increase cellular uptake and/or facilitate targeting of the compounds to DNA [6]. The latter approach involves the incorporation of a functional group into the platinum complex that interacts or intercalates with DNA. Numerous conjugates have been prepared in which the Pt moiety has been tethered to high-affinity nucleic acid ligands, such as doxorubicin [7], acridine [8], amines or peptides [9], anthraquinones [10] and short oligonucleotides [11]. In particular, a mixed platinum(II) complex with doxorubicin demonstrated antitumor activity against a variety of tumor cell lines, including doxorubicin- and cisplatin-resistant cell lines. Moreover, in contrast to the highly toxic doxorubicin/cisplatin combination, the doxorubicin–platinum complex was not associated to an increase in toxicity [7].

As part of our program aimed to advance DNA as a drug target, we were interested in devising novel platinum containing dual

* Corresponding author. Tel.: +39 (2)50316818; fax: +39 (2)50316801.
E-mail address: sabrina.dallavalle@unimi.it (S. Dallavalle).

0223-5234/$ – see front matter © 2013 Elsevier Masson SAS. All rights reserved.
http://dx.doi.org/10.1016/j.ejmech.2013.02.022

compounds that interacted in an effective way with DNA and in addition accomplished the requirements of solubility in the body fluids and improved cellular uptake. In this context, a promising approach seemed to be the conjugation of platinum to analogues of the natural antitumor compound camptothecin (CPT).

CPTs [12] are widely used for the treatment of human cancers [13]. They exhibit a unique mechanism of action because they target the topoisomerase I (Topo I), forming a ternary complex with the enzyme and DNA [14]. Stabilization of the cleavable complex and collision with the replication fork results in lethal double-strand breaks during DNA replication [15]. On the basis of this mechanism of action, the reversibility of drug-target interaction represents a limitation that results in resistance of slowly growing tumors. Intensive efforts in medicinal chemistry over the past decades have provided a large number of CPT analogues, of which topotecan (TPT) and irinotecan (prodrug of SN-38, Chart 2) are those so far approved for the clinical therapy [16].

Given the chemical interest of these agents [17], we planned to incorporate the two active compounds in a single "hybrid" molecule with the intention of exerting dual action and/or increase the drug-target interaction. The potential advantages of using CPT–Pt conjugates are multiple. On one hand, they could promote adequate cellular accumulation and nuclear localization of the Pt(II)-complex by virtue of the hydrophobicity of CPTs. On the other hand, the incorporation of a chemical function able to covalently bind to DNA, like a Pt moiety, could stabilize the CPT–DNA–enzyme ternary complex, thereby improving the drug-target interaction.

In the present study, we describe the synthesis, molecular modeling and biological evaluation of CPT–Pt complexes with different Pt-containing linkers. To the best of our knowledge, there are no examples in the literature of diaminedichloro-platinum (II) complexes tethered to CPT analogues.

2. Results and discussion

2.1. Chemistry and molecular modeling

The following criteria have guided the design of the CPT–Pt(II) conjugates: a) a CPT moiety substituted in a suitable position to maintain cytotoxic activity; b) a linker between the Pt center and the CPT skeleton, chosen to ensure enough conformational flexibility while maintaining proximity of the reactive metal center to the DNA-selective scaffold; c) a chelating diamine selected to secure Pt(II) coordination to the CPT moiety.

Recently, a series of CPTs substituted in position 7 have been synthesized in our laboratory. The compounds exhibited potent cytotoxic activity *in vitro* and *in vivo* comparable or superior to TPT [18–20]. The highest activity was shown by oxyiminomethyl derivatives, even when bulky [19] and long-chain [20] substituents were introduced. Some compounds gave promising results in preclinical [21] and clinical [22] studies. In contrast, incorporation of the same groups in position 9 caused a drop in cytotoxic activity [23].

For this reason, (*E*)-7-oxyminomethyl CPTs were selected for conjugation to Pt(II) [19]. Initially, we focused on the most promising 7-substituted compound in our hands, **3a** (Fig. 1). As the molecule is characterized by a terminal amino group, we planned to link the CPT moiety to Pt(II) through an amide bond. Thus, the synthesis of compound **1a** (Fig. 1), designed as our first conjugate, was devised to proceed by coupling of **3a** with 2,3-diaminopropionic acid followed by complexation of the derived diamine (**2a**) with a suitable platinum salt.

Prior to start the synthesis, we studied the binding mode of compound **1a** to the Topo I covalent complex with DNA [24]. A two-step protocol was used to obtain a better estimate of the orientation of the ligands within the binding site. First, the non-platinated ligands were correctly placed within the binding site using the molecular docking technique. On the basis of the geometry of interaction thus obtained, the platinated ligands were built and analyzed using the QM/MM approach. To gain insight into the role of the linker on the interaction with the target, we also modeled the binding of a series of derivatives **1** with different carbon chain length ($n = 1$–4). Molecular modeling showed that the compound with six carbons ($n = 3$, **1b**) demonstrated the best interactions. Thus, for the sake of clarity, here we describe only the target-drug interactions of compound **1b** compared to **1a**.

The intercalation binding site for all of the studied compounds was located between the +1 (upstream) and −1 (downstream) base pairs of the uncleaved strand, which effectively "open" the DNA duplex. Comparative analysis of the best poses obtained for the four non-platinum-containing compounds (**2a**–**b**, **3a**–**b**) revealed their common behavior of intercalating at the site of DNA cleavage, forming base-stacking interactions with both the −1 and +1 base pairs. There is evidence of two direct hydrogen bonds between the Asp^{533} and Arg^{364} residues of the enzyme and the planar skeleton of the investigated derivatives, in perfect agreement with the CPT–DNA complex structure [24]. The greatest differences were found by analyzing the behavior of the side chains. For **2a**, the side chain was too short and allows only a partial interaction with the DNA duplex, leading one of the two amino groups to interact with O^6 and N^7 of G^{11}, whereas the immine nitrogen interacts weakly with N^6A^{113}. For both **2b** and **3b**, the greater length of their side chains allows them to interact more efficiently with the DNA duplex. The amino group of **3b** forms three strong hydrogen with N^7G^{11}, whereas **2b** forms a hydrogen bond to N^6A^{113}, two between the amino group and O^6G^{12} and the last with N^7G^{11}. The interactions between derivatives **2a** and **2b** and the DNA-Topo I complex are

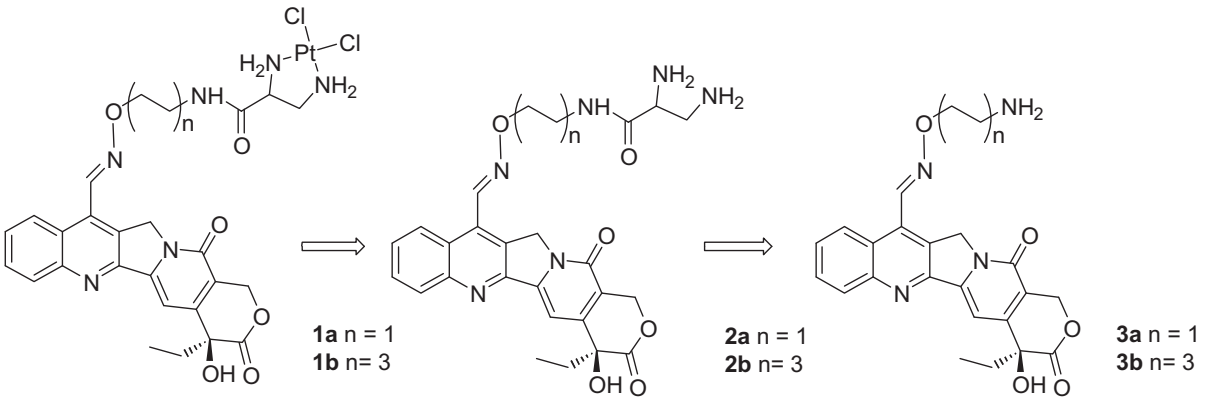

Fig. 1. Retrosynthetic approach to compounds **1**.

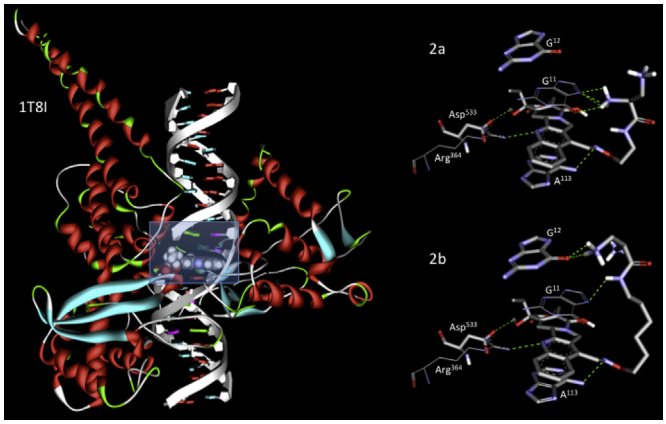

Fig. 2. Interactions between the derivatives (**2a** and **2b**, on the right) and the experimental DNA–Topoisomerase I complex (left). The binding site is located inside the region delimited by the white rectangle (left) and the dotted green lines (right side) represent the intermolecular hydrogen bonds. (For interpretation of the references to colour in this figure legend, the reader is referred to the web version of this article.)

given in Fig. 2 (together with the experimental DNA-Topo I structure (PBD code 1T8I)), where the interactions listed as dotted green lines represent the intermolecular hydrogen bonds.

Orientations of the systems described above (**2a** and **2b**) were used to assemble the two Pt complexes (**1a** and **1b**), which were further analyzed using the QM/MM mixed approach on the platinated complexes. This QM/MM mixed approach allowed us to obtain a better and more complete description of the interactions of the two Pt complexes with the DNA-Topo I system, as well as an evaluation of the structural changes induced in the complex by the binding of ligands **1a** and **1b**. Major differences were observed at the level of the side chain, whereas the CPT ring maintained its position inside the DNA-Topo I system (Fig. 3).

The compound with the longer spacer (**1b**) is more effective in its interaction with the DNA duplex than the one with the shorter side chain (**1a**). Both complexes are stabilized by the formation of two hydrogen bonds between O^6G^{12} and an amino group bound to the platinum atom that lies in the square planar coordination plane with a small distortion of the Pt–N^7 bond due to the destacking of the bases. Compound **1b** is further stabilized by two interactions with N^7G^{11} and N^6A^{113}, the same as those previously discussed for **2b**. Indeed, the complex formation induces a distortion of the DNA duplex, with a partial destacking of the nucleotide bases, which is less marked in the case of compound **1b**. The shift of G^{12} in the complex with **1a** is significantly larger (7.1 Å) than in the complex with **1b** (5.4 Å), in poor agreement with the guanine position in the crystal structure. Moreover, the hydrophobic face of the guanine

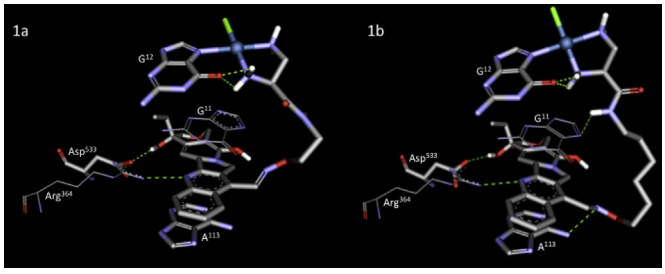

Fig. 3. Interactions between the Pt-derivatives (**1a** and **1b**) and the experimental DNA–topoisomerase I complex. The main structural changes induced in the complex by the presence of platinum were observed at the level of the side chain, whereas the CPT ring maintained its position inside the DNA–topoisomerase I system. Again, the dotted green lines represent the intermolecular hydrogen bonds. (For interpretation of the references to colour in this figure legend, the reader is referred to the web version of this article.)

base for **1a** is even more solvent exposed than for **1b**, giving rise to an additional source of instability of the **1a** complex.

It should be noted that in Figs. 2 and 3, the best poses for derivatives **1** and **2** with only *S* absolute configuration at the stereogenic center on the diamine moiety are reported. The best poses for the corresponding *R* diastereomers did not show striking differences with regard to chirality, indicating that the stereochemistry of the diamine moiety does not seem to play a role in the interaction with DNA.

On the basis of molecular modeling results, the synthesis of compounds **1a** and **1b** was carried out.

Compound **1a** was prepared from the corresponding 7-oxyminomethylCPT **3a** [19], which in turn was obtained from 7-formylCPT (**4**). The oxime was then condensed with N,N-bis-*t*-butoxycarbonyl-2,3-diaminopropanoic acid in the presence of WSC and HOBt as condensing agents. The Boc-diamine **5a** was quantitatively deprotected with TFA in CH_2Cl_2 to obtain the bistrifluoroacetate **6a**. Reaction with K_2PtCl_4 [25] afforded **1a** in 69% yield (Scheme 1).

The synthesis of compound **1b** required the preparation of the longer-chain hydroxylamine **8** (Scheme 2). Protection of 6-aminohexanol with $(Boc)_2O$, followed by Mitsunobu reaction with N-hydroxyphthalimide, afforded compound **7**. Hydrazinolysis and subsequent deprotection from the Boc group with 5.9 M HCl at 0 °C afforded hydroxylamine **8** hydrochloride. Condensation with 7-formylCPT (**4**) by refluxing in ethanol in the presence of pyridine afforded oxime **3b**.

Following the same synthetic approach described for compound **1a**, the bistrifluoroacetate **6b** was obtained in 65% overall yield from **3b**. Disappointingly, in this case the reaction with K_2PtCl_4 gave compound **1b** in low yield and unsatisfactory purity, due to a troublesome separation of the desired compound from the salt **6b**. Thus, a different strategy was followed. The *cis*-dichlorobis(diaminopropionic acid hydrochloride) platinum (II) complex was first prepared in high yield by reacting 2,3-diaminopropionic acid hydrochloride with K_2PtCl_4 in H_2O [26] and then condensed with **3b** to give **1b** in 89% yield (Scheme 2).

2.2. Antiproliferative activity studies

The antiproliferative effect of the derivatives **1a**–**b** and **6a**–**b** was determined at 1 h exposure on different human tumor cell lines, including cell lines resistant to TPT and platinum compounds (Table 1). TPT and cDDP were used as reference drugs. All the tested compounds were generally more potent than cDDP on all the selected cell lines, including those resistant to cDDP, oxaliplatin and TPT. In contrast, a comparison between the new CPT–Pt derivatives and TPT revealed cell line-dependent drug potency. A superior cytotoxicity with respect to TPT was evidenced for **1b** and **6b** on the H460 cell line, since **6a** and **1a** are less potent than TPT. All the compounds were less potent that TPT in the squamous cell carcinoma A431 cell line, including the corresponding sublines resistant to TPT (A431/TPT) and cDDP (A431/Pt). The compounds were less potent than TPT in the osteosarcoma U2OS cell line and, with the exception of **1b**, such behavior was observed also in the corresponding cDDP-resistant variant (U2OS/Pt). A general reduced potency with respect to TPT was observed in ovarian carcinoma IGROV-1 and A2780 cell lines. This was also evident in the corresponding cDDP and oxaliplatin-resistant sublines with the exception of **1b** in IGROV-1/Pt and **1b** and **6b** in IGROV-1/OHP cells.

As regards the resistance index (ratio between IC_{50} values of resistant and sensitive cells), the contribution of the Pt(II) complex was demonstrated by the reduced resistance indexes observed for CPT–Pt derivatives with respect to cDDP and TPT in several human tumor cell lines. The resistance index of CPT–Pt (**1a** and **1b**) was

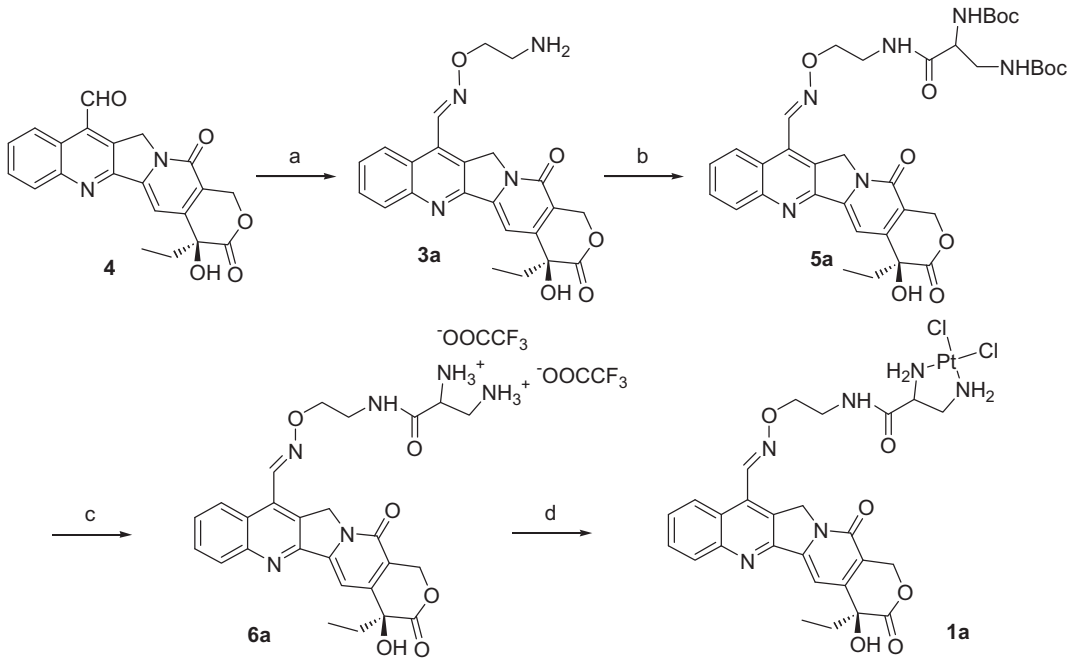

Scheme 1. Reagents and conditions: (a) $H_2N{-}O{-}CH_2CH_2NH_2{\cdot}2HCl$, ethanol, Py, reflux, 1 h, 63%; (b) N,N-bis-*t*-butoxycarbonyl-2,3-diaminopropanoic acid, WSC, HOBt, DIPEA, DMF, rt, 2.5 h, 77%; (c) TFA/CH_2Cl_2 1:1, from 0 °C to rt, 3 h, quantitative; (d) K_2PtCl_4, H_2O, N_2, rt, 3h, 69%.

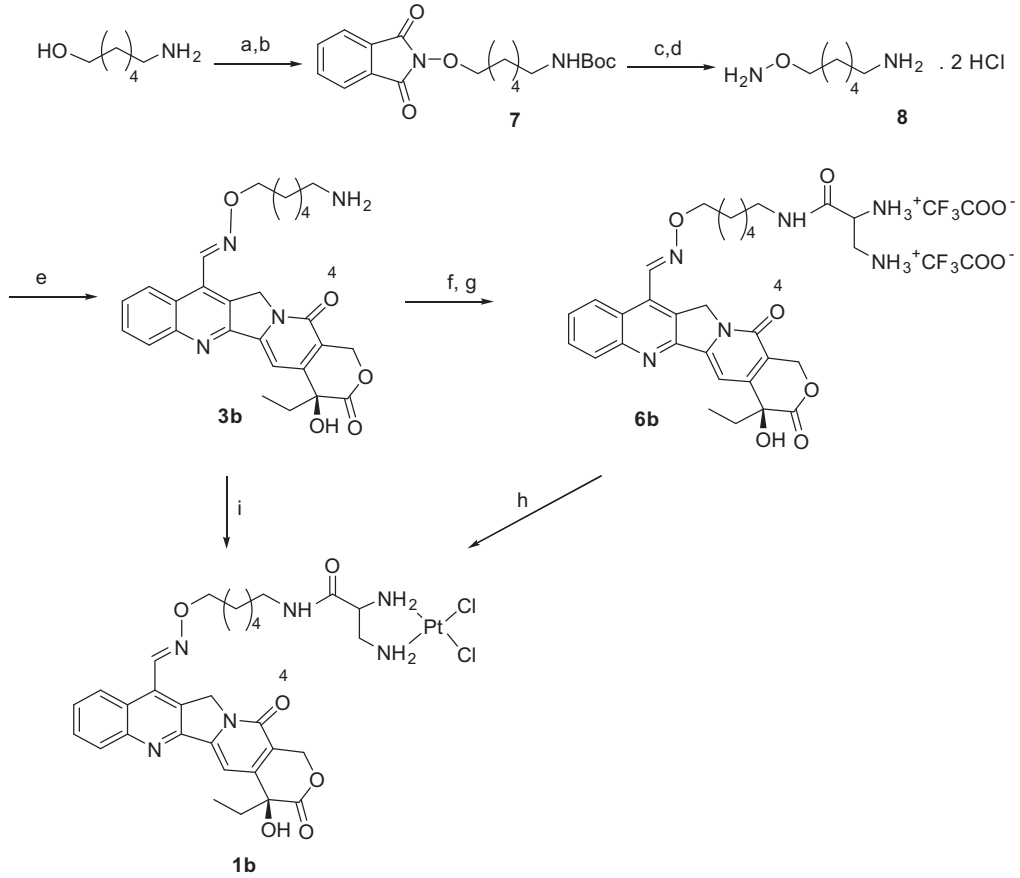

Scheme 2. Reagents and conditions: (a) $(Boc)_2O$, CH_2Cl_2, rt, overnight, 99%; (b) N-hydroxyphthalimide, triphenylphosphine, DIAD, THF, from 0 °C to rt, 1 h, 50%; (c) hydrazine hydrate, methanol, reflux, 1 h, quantitative; (d) HCl 5.9 M in ethyl acetate, ethyl acetate, 0 °C, 1 h, 97%; (e) **4**, Py, ethanol, reflux, 1 h, 77%; (f) N,N-bis-*t*-butoxycarbonyl-2,3-diaminopropanoic acid, WSC, HOBt, DIPEA, DMF, rt, 2.5 h, 65%; (g) TFA/CH_2Cl_2 1:1, from 0 °C to rt, 3 h, quantitative; (h) K_2PtCl_4, H_2O, N_2, rt, 3h, 20%. (i) cis-dichlorobis[(*d*,*l*)-diaminopropionic acid hydrochloride]platinum(II), EDC, TEA, DMF, rt, overnight, 89%.

Table 1
Cellular sensitivity of human tumor cell lines to CPT derivatives.[a]

Cell line	TPT	cDDP	**6a**	**1a**	**6b**	**1b**
H460	1.37 ± 0.34	22 ± 6.3	6.47 ± 2.82	4.1 ± 0.59	0.44 ± 0.017	0.4 ± 0.016
U2OS	0.48 ± 0.4	20.5 ± 9.2	4.2 ± 2.26	5.39 ± 2.4	1.36 ± 0.34	1.09 ± 0.54
U2OS/Pt	2.34 ± 0.86 (4.87)	107.8 ± 24 (5)	10.9 ± 4.44 (2.6)	14.2 ± 5.6 (2.6)	2.59 ± 1.58 (1.9)	0.82 ± 0.25 (0.75)
A431	0.075 ± 0.067	19.57 ± 1.37	0.99 ± 0.35	1.68 ± 0.29	0.28 ± 0.099	0.185 ± 0.035
A431/TPT	0.29 ± 0.01 (3.86)	16.84 ± 2.19 (0.86)	8 ± 1.4 (8)	14.2 ± 0.28 (8.4)	2.87 ± 1.94 (10.3)	1.23 ± 0.89 (6.6)
A431/Pt	0.27 ± 0.29 (3.6)	64.6 ± 7.6 (3.3)	4.27 ± 1.07 (4.3)	3.79 ± 1.7 (2.25)	0.72 ± 0.176 (2.57)	0.67 ± 0.19 (3.62)
IGROV-1	1.03 ± 0.8	14.8 ± 2.54	17.8 ± 4.5	5.79 ± 0.29	2.24 ± 0.3	1.24 ± 0.077
IGROV-1/Pt	3.9 ± 0.96 (3.9)	211 ± 19 (14)	11.8 ± 1.42 (0.66)	14.2 ± 10.2 (2.5)	4.1 ± 2.14 (1.8)	3.03 ± 1.32 (2.4)
IGROV-1/OHP	10.9 ± 1.34 (10.5)	120.8 ± 20 (8)	28 ± 7.5 (1.57)	15.8 ± 2.6 (2.7)	2.38 ± 0.18 (1.06)	3.17 ± 0.75 (2.6)
A2780	0.036 ± 0.0035	4.35 ± 0.49	0.69 ± 0.44	2.16 ± 0.23	0.08 ± 0.028	0.22 ± 0.064
A2780/CP	0.275 ± 0.01 (7.6)	41.5 ± 9.2 (9.5)	2.55 ± 0.35 (3.7)	4.8 ± 1.4 (2.2)	0.79 ± 0.45 (9.8)	0.73 ± 0.31 (3.3)

[a] Cell sensitivity to drug was assessed by growth-inhibition assay. Twenty-four hours after seeding, cells were exposed to drug for 1 h and then, after an additional 72 h, counted using a cell counter. The reported value is the IC_{50} expressed in μM (drug concentration inhibiting growth by 50%). In parenthesis is reported the resistance index (ratio between IC_{50} values of resistant and sensitive cells). Data represent mean values ± SD from at least 3 independent experiments.

higher than that of cDDP and TPT in A431/TPT cells. Conversely, a reduced resistant index with respect to TPT and cDDP was observed for the two hybrid compounds in A431/Pt, U2OS/Pt, IGROV-1/Pt, IGROV-1/OHP and A2780/CP cells.

It is noteworthy that the most active derivative **1b** was effective in overcoming cDDP resistance in osteosarcoma cDDP-resistant U2OS cells (Table 1 and Fig. 4).

To clarify the role of the Pt(II) complex in drug activity, the ratio between the IC_{50} of compounds not containing Pt and the IC_{50} of compounds containing Pt (**6a**/**1a** or **6b**/**1b**) was considered. A ratio higher than 1 indicates the positive effect produced by the Pt atom. As reported in Fig. 4, the role of the Pt atom appears more important for the potency of **1b** than for **1a**. Indeed, considering the 11 cell lines evaluated, the ratios were <1 in six cell lines for **6a**/**1a** and only in two cell lines for **6b**/**1b**.

2.3. Drug combination studies

Drug combination experiments using platinum compounds with CPTs are widely documented [27]. Synergism was evidenced in various human tumor cell lines [27]. Indeed, the presence of Pt–DNA adducts in the substrate DNA inhibited Topo I activity, whereas it enhanced CPT action on the cleavable complex [28]. The effect of the combination of cDDP and our derivatives (**6a**–**b**) on antiproliferative activity was evaluated on the H460 cell line (Fig. 5). To this purpose, cells were simultaneously exposed for 1 h to increasing concentrations of CPTs and to subtoxic concentration (10 μM) of cDDP (Fig. 5). The data demonstrated that, as for the combination of cDDP with TPT, the combination of **6a**–**b** with cDDP resulted in a synergistic interaction, thus supporting the rational of joining the two moieties into a single molecule.

2.4. Topoisomerase I-dependent DNA cleavage assay

Topo I-mediated DNA cleavage experiments were performed to investigate the ability of the new compounds to stimulate DNA damage. SN38 was used as reference compound. As reported in Fig. 6, a dose-dependent precipitation of labeled DNA in the wells was observed for CPT–Pt derivatives (**1a** and **1b**). This behavior was drug- and enzyme-dependent since it was not observed in the presence of cDDP, **6b**, or in the absence of Topo I.

Stabilization of the ternary cleavable complex was evaluated by adding a high salt concentration (0.6 M NaCl) after 30 min of incubation in the presence of the tested compound. The high salt concentration favors the dissociation of the drug–enzyme–DNA complex, thus producing evidence of the stability of the ternary

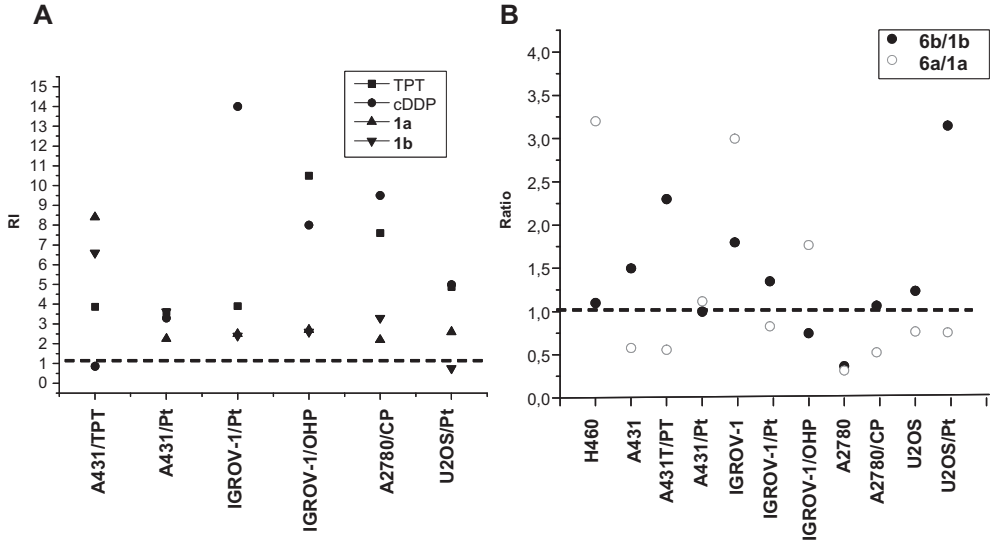

Fig. 4. (A) Graphic representation of the resistance indexes observed in the tested cell lines. The ratio between IC_{50} values of resistant and sensitive cells is reported for **1a** and **1b**. The resistant indexes of TPT and cDDP are reported for comparison. (B) Graphic representation of the ratio between the IC_{50} of the compound not containing Pt (**6b** or **6a**) and the IC_{50} of the compound containing Pt (**1b** or **1a**). A ratio higher than 1 (dashed line) indicates the positive effects produced by the Pt atom for drug potency.

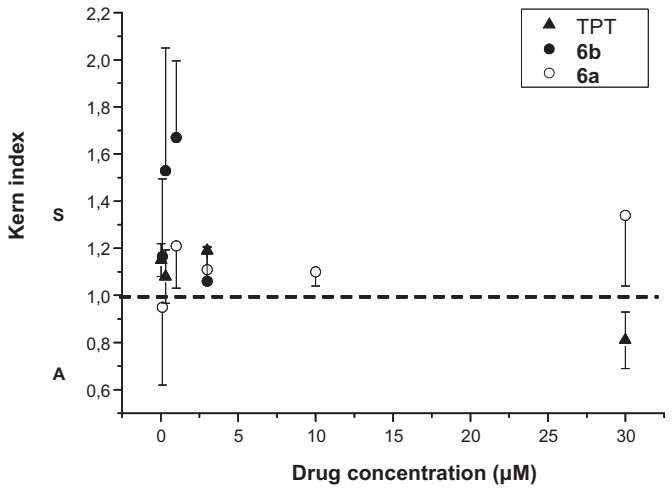

Fig. 5. Interaction between camptothecins and cDDP. Antiproliferative activity of the combination was determined after a 1 h exposure to the camptothecin and cDDP using a cell counter. Dose-response curves for each CPT were determined in the presence of subtoxic concentrations of cDDP (10 μM; i.e., under conditions that did not produce antiproliferative effects of the cDDP). The combination index was calculated according to the method of Kern. S, synergism; A, antagonism.

complex. The stability of the cleavage complex was evaluated at 1 μM drug concentration. It was not possible to evaluate the stability of the cleavable complex at 10 μM drug concentration since the accumulation of the labeled DNA into the wells was not reversed (data not shown). The cleavage persistence evaluated at 1 μM indicated that CPT–Pt **1b** and **1a** induced a persistent cleavage

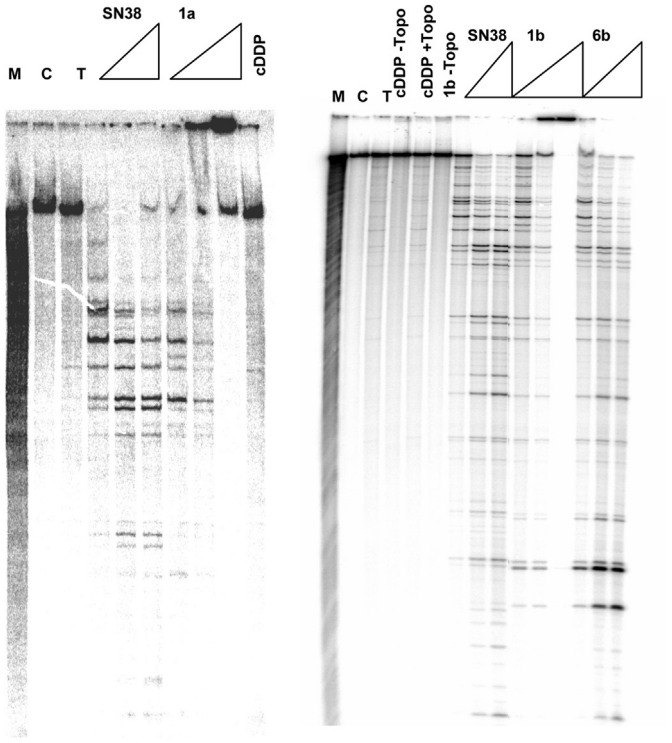

Fig. 6. Topoisomerase I-mediated DNA cleavage by SN38 and CPT derivatives. Samples were reacted with 1, 10 and 50 μM drug at 37 °C for 30 min. Reaction was then stopped by adding 0.5% SDS and 0.3 mg/ml of proteinase K and incubating for 45 min at 42 °C before loading on a denaturing 8% polyacrylamide gel. C, control DNA; T, reaction without drug; M, purine markers.

stability with respect to SN38. Such behavior was less evident when CPT–Pt compounds were compared with the corresponding derivatives lacking Pt (**6a** and **6b**) (Fig. 7).

2.5. Drug uptake and DNA platination

Drug uptake and DNA platination were evaluated in H460 cells exposed for 1 h to equitoxic (IC_{50} cDDP = 22 μM; **1a** = 4.1 μM; **1b** = 0.4 μM) or equimolar (0.4 μM) concentrations of compounds. cDDP was used as reference drug. As reported in Fig. 8A, at equitoxic concentrations a marked cellular uptake of **1a** was observed. It is noteworthy that the uptake of **1b** was comparable to that of cDDP, in spite of its 55-fold lower concentration. As regards the exposure to equimolar drug concentration (0.4 μM), a significantly higher cellular Pt accumulation was evidenced for **1a** ($P < 0.02$) and **1b** ($P < 0.01$) with respect to cDDP (Fig. 8B).

DNA platination was studied in H460 cells exposed for 1 h to equitoxic (IC_{50}) concentrations of compounds. Pt–DNA adducts were revealed in the DNA extracted from cells treated with both **1a** and **1b** (Fig. 8C). DNA-bound Pt was significantly higher in cells exposed to cDDP than **1a** and **1b** ($P < 0.02$). The finding is expected, because the low potency of cDDP required the use of substantially higher concentrations (IC_{50} cDDP = 22 μM). In contrast, the exposure of H460 cells to equimolar concentration of drugs (0.4 μM) resulted in DNA platination only in cells treated with **1b** (data not shown).

2.6. Viability and DNA platination of yeast cells expressing human DNA topoisomerase I

The *S. cerevisiae* JN2-134 strain, which lacks endogenous DNA Topo I, was used. Yeast cells transformed with the empty vector (pEMBLyex4) or with the same vector containing the entire ORF of the human DNA Topo I (pEZ-2hTop1) were treated with CPTs (**1a**–**b**, **6a**–**b**) for 24 h and then plated according to the yeast spot test (Fig. 9). CPT and cDDP were used as references. cDDP exhibited similar growth inhibitory potency on both pEMBLyex4 and pEZ-2hTop1 transformed yeasts, indicating that cDDP potency was unaffected by the presence/absence of Topo I. Conversely, cell growth of yeast cells expressing human Topo I was affected by the exposure to CPTs (**1a**–**b**, **6a**–**b**). No important change in cell growth was observed for yeast cells transformed with the empty vector and treated with CPTs. Interestingly, a significant increase ($P < 0.01$) in DNA platination was documented in yeasts expressing human Topo I and treated with CPT–Pt with respect to yeasts transformed with empty vector (Fig. 9B). Although less relevant, a significant change ($P < 0.02$) in the amount of Pt–DNA adducts was also observed for transformed yeasts treated with cDDP.

2.7. Effect of DNA Topoisomerase I on the formation of Pt–DNA adducts

CPT derivatives (**1a**–**b**, **6a**–**b**) were tested for their capability to bind the DNA by evaluating the migration of pCMV6neo plasmid in agarose gel electrophoresis after drug exposure (Fig. 10). In comparison to cDDP and SN38, which did not produce any effect on DNA migration, the exposure of plasmid DNA to **1a** revealed a significantly reduced migration of the vector. Such behavior was likely dependent on the major capability of **1a** to produce Pt–DNA adducts. The effect was less marked for **1b**. Moreover, the simultaneous exposure of pCMV6neo plasmid to Topo I and **1a** or **1b** produced DNA accumulation in the wells, thus resembling that observed in cleavage assays. Such behavior was dependent on the presence of Topo I, since it was not observed in the absence of enzyme or in the presence of human serum albumin (BSA). Interestingly, degradation of the protein by SDS and proteinase K before loading on agarose gel

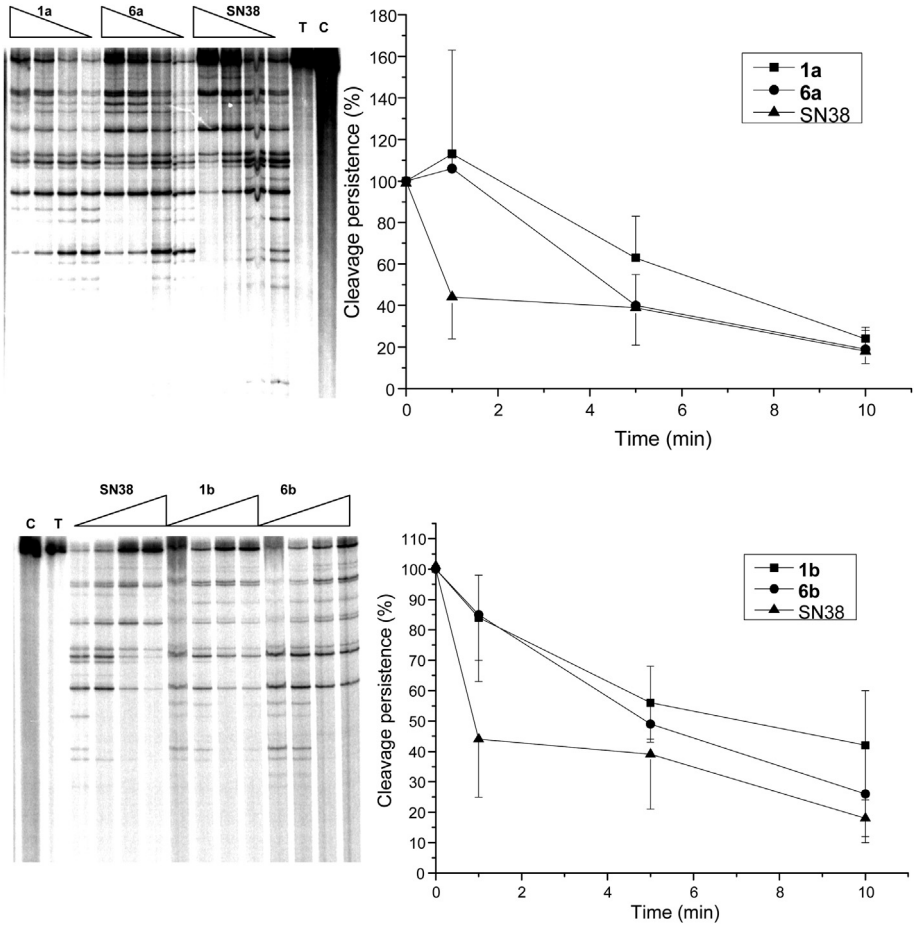

Fig. 7. Persistence of topoisomerase I-mediated DNA cleavage in the presence of SN38 and camptothecin derivatives. Time-course analysis of DNA cleavage induced by SN38 and camptothecin analogs. The samples were reacted for 30 min with 1 μM drug. DNA cleavage was then reversed by adding 0.6 M NaCl. The 100% value refers to the extent of DNA cleavage at 30 min of incubation. C, control DNA; T, reaction without drug. Cleavage persistence was measured by densitometric analysis. Data represent mean values from 3 independent experiments.

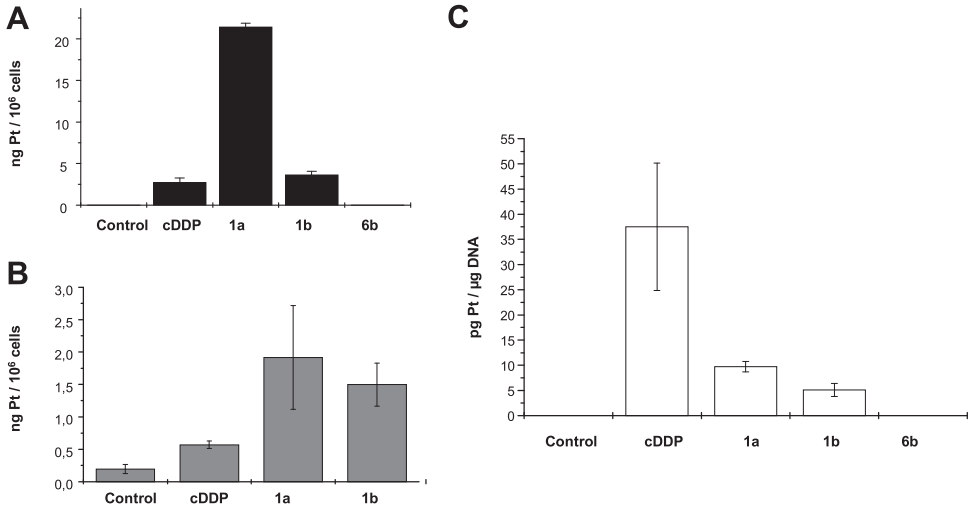

Fig. 8. Cellular Pt accumulation and DNA platination in the H460 cell line. Platinum accumulation was determined after a 1 h exposure to equitoxic (IC_{50}) (A) and equimolar (0.4 μM) (B) concentrations of cDDP and CPT derivatives. (C) DNA-bound platinum after a 1 h exposure to equitoxic concentration (IC_{50}) of cDDP and camptothecin derivatives. Accumulation was assessed by atomic absorption spectroscopy, and DNA platination was measured by inductively coupled plasma mass spectroscopy. Mean values (±SD) of triplicate determinations are shown.

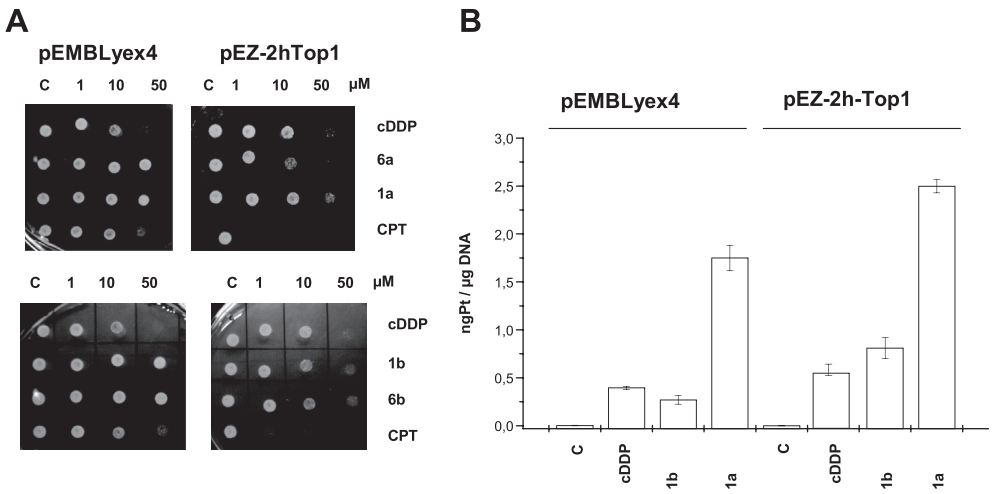

Fig. 9. (A) sensitivity of *S. cerevisiae* JN2-134 strain in spot test. Yeast cells transformed with the empty vector (pEMBLyex4) or with the same vector containing the entire ORF of the human DNA topoisomerase I (pEZ-2hTop1) were used. Yeasts were grown to an A_{595} of 0.3 and then treated for 24 h with CPT derivatives at 1, 10 and 50 μM. Aliquots of 10 μl were spotted onto plates and incubated for 3 days at 30 °C. Two references (CPT and cDDP) were included in the test. (B) DNA-bound platinum after overnight exposure of the transformed JN2-134 strain to 50 μM cDDP and CPT derivatives. After treatment, genomic DNA was extracted and Pt–DNA adducts were measured by inductively coupled plasma mass spectroscopy. Mean values (±SD) of triplicate determinations are shown.

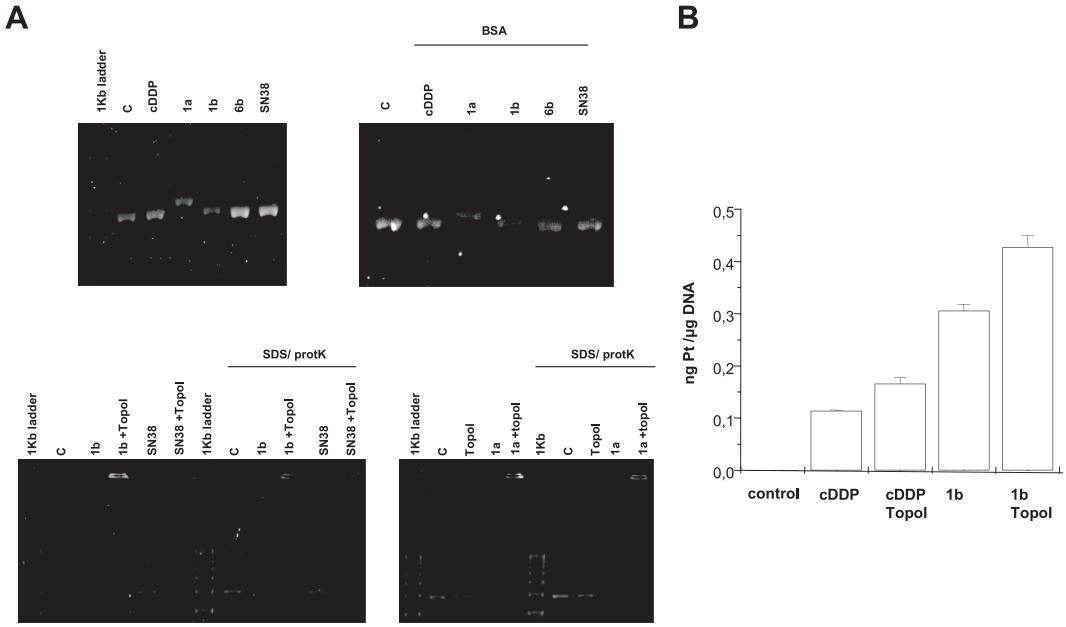

Fig. 10. (A) DNA binding of CPT containing Pt. EcoRV linearized pCMV6neo plasmid (200 ng) and CPT analogues (50 μM) were incubated for 1 h at 37 °C before loading on 1% agarose gel. Where indicated, before loading on agarose gel, samples were treated with 0.5% SDS and 0.3 mg/ml of proteinase K. (B) Platination of pCMV6neo vector after exposure to CPT derivatives. pCMV6neo plasmid (10 μg sample) was treated for 1 h at 37 °C with 50 μM of cDDP or **1b** in the presence or absence of topoisomerase I. DNA concentration was determined spectrophotometrically and platinum content was measured by flameless atomic absorption spectroscopy.

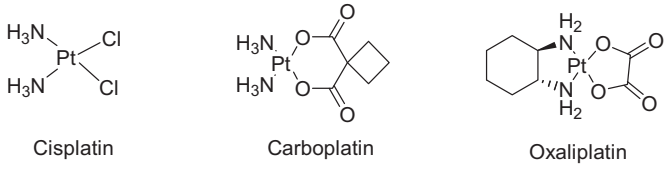

Chart 1. Chemical structures of the clinically approved platinum dugs: cisplatin, carboplatin and oxaliplatin.

Table 2
Antitumor activity of **1b** against human H460 tumors xenografted s.c. in athymic nude mice.

Compound	Days of treatment	Dose (mg/kg)	TVI% (20)[a]	BWL%[b]	Tox[c]
1b	3, 7, 11, 15	25	82**	0	0/6
cDDP	3, 10, 17	5	58**	11	1/5
Irinotecan	3, 7, 11, 15	60	88**	8	0/8

**$P < 0.01$ by two-tailed Student' t test vs control mice.
[a] Tumor volume inhibition % in treated over control mice; in parentheses the day it was assessed. Tumor fragments were implanted in both flanks at day 0. Treatment started when tumors were just palpable. CPTs were administered i.v. according to the q4dx4 schedule. cDDP was administered i.v. at the maximum tolerated dose and according to the schedule q7dx3.
[b] Body weight loss % induced by drug treatment; the highest change is reported.
[c] Dead/treated mice.

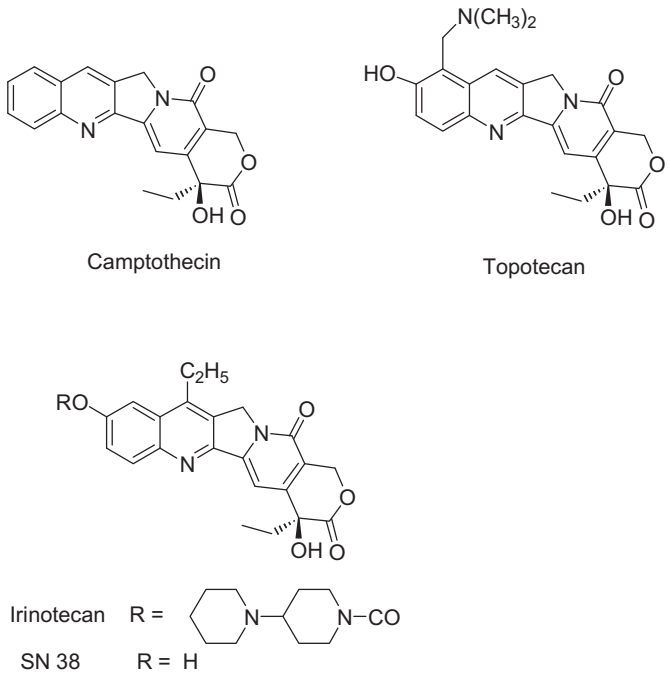

Chart 2. Chemical structures of camptothecin and of the two clinically approved derivatives topotecan and irinotecan. The structure of SN38, the active metabolite of irinotecan, is reported.

produced a different behavior depending on the compound. No change in DNA migration was evidenced with respect to unproteolized sample for plasmid exposed to **1b**, whereas a migration similar to the control was obtained when DNA treated with **1a** and Topo I was exposed to SDS/proteinase K before loading.

To evaluate the effect of Topo I on platination of the plasmid DNA, pCMV6neo was exposed to **1b** or cDDP in the presence and absence of Topo I in a cell-free system. As reported in Fig. 10B, the Pt–DNA adducts were significantly increased by the addition of purified human Topo I in the presence of both cDDP ($P < 0.05$) and **1b** ($P < 0.02$).

2.8. In vivo antitumor activity

On the basis of the promising results observed *in vitro*, compound **1b** was selected for further preclinical development. Mice bearing non-small cell lung cancer H460 carcinoma tumor xenograft were treated with **1b** administered intravenously (i.v.) according to the intermittent q4dx4 schedule (Table 2). Compound **1b** exhibited antitumor activity comparable to that of irinotecan and higher than that of cDDP, both delivered at their maximum tolerated doses. Considering the toxicity profile, **1b** was well tolerated (no lethal toxicity and no body weight loss) with respect to cDDP (1/5 toxic deaths).

3. Conclusions

Platinum drug administration is associated with dose-limiting side effects, off-target effects and relatively poor pharmacokinetic profiles. In particular, the low cellular uptake and the rapid metabolic inactivation of platinum compounds imply that the amount of active drug reaching the target is low. As regards CPTs, the reversibility of the DNA cleavage may represent a limitation of drug efficacy, resulting in resistance of slowly growing tumors. In an attempt to overcome such drawbacks, hybrid 7-oxyiminomethyl CPTs containing a Pt(II) complex were synthesized. Molecular modeling studies evidenced that the CPT moiety of the hybrid drugs overlapped TPT in the cleavable complex, independently of the absolute configuration of the stereogenic center on the diamine moiety. The most efficient interaction with duplex DNA was observed for compound **1b**, thus supporting a critical role of the linker to provide drug–DNA interaction. CPT–Pt derivatives were effective antiproliferative agents, with potency similar/superior to TPT and in general more potent than cDDP. The potential advantage of the Pt(II) complex was also supported by the reduced resistance indexes observed for CPT–Pt derivatives with respect to cDDP and TPT in several human tumor cell lines. It is noteworthy that the most active derivative **1b** was effective in overcoming cDDP resistance in osteosarcoma cDDP-resistant U2OS cells. More importantly, CPT–Pt exhibited activity both as a Topo I poison and as a DNA-platinating molecule, thus indicating that the conjunction of the two components in a one hybrid molecule did not negatively impact on their properties as single drugs. Interestingly, results obtained in a cell-free system and in experiments involving yeast cells documented two relevant findings produced by the presence of Topo I: i) DNA platination produced by the CPT–Pt molecules was increased in the presence of Topo I, and ii) the presence of Topo I, but not BSA, produced a dose-dependent accumulation of DNA in the wells of agarose and acrylamide gels, thus evoking a network organization involving DNA, CPT–Pt and Topo I. It could be speculated that the network effect observed at a high concentration might be the result of CPT–Pt acting outside, rather than inside, the active site of Topo I. Thus, a scenario in which the Pt atoms form covalent bounds linking the DNA and the Topo I outside the active site should be considered as a possible alternative/additional mechanism of drug action. This aspect remains to be properly investigated.

Concerning antitumor activity, preliminary *in vivo* data indicated that compound **1b** was well tolerated and exhibited promising antitumor potency, comparable to that of irinotecan and superior to that of cDDP. The widely used combinations of CPTs with platinum compounds exhibit synergism in terms of both efficacy and toxicity. Thus, the good profile of tolerability of the CPT–Pt complex supports additional therapeutic advantages over the drug combinations.

In conclusion, results of the study provide evidence that CPT and a Pt(II) complex joined in a single molecule via an oxyiminomethyl linker could be considered a new class of effective antitumor compounds.

4. Experimental section

4.1. Chemistry. General methods

All reagents and solvents were reagent grade or were purified by standard methods before use. Melting points were determined in open capillaries. NMR spectra were recorded with a Bruker AMX 300 spectrometer using TMS as an internal standard. Chemical shifts are given in ppm (δ). Mass spectra were recorded with a Fourier transform ion cyclotron resonance (FT-ICR) mass spectrometer APEX II & Xmass software (Bruker Daltonics)-4.7T Magnet (Magnex). The elemental analyses were recorded with a CARLO ERBA EA 1108 instrument. Solvents were routinely distilled prior to use; anhydrous tetrahydrofuran (THF) and ether (Et_2O) were obtained by distillation from sodium–benzophenone ketyl; dry dichloromethane was obtained by distillation from phosphorus pentoxide. All reactions requiring anhydrous conditions were performed under a positive nitrogen flow, and all glassware were oven dried and/or flame dried. Isolation and purification of the compounds were performed by flash column chromatography on silica gel 60 (230–400 mesh). Analytical thin-layer chromatography (TLC) was conducted on TLC plates (silica gel 60 F_{254}, aluminum foil).

4.1.1. {2-tert-Butoxycarbonylamino-1-[2′-(camptothecin-7-ylmethyleneaminooxy)ethylcarbamoyl]ethyl}carbamic acid tert-butyl ester (**5a**)

To a solution of N,N-bis-t-butoxycarbonyl-2,3-*d*,*l*-diaminopropanoic acid [25] (134 mg, 0.441 mmol) in anhydrous DMF (6.6 mL) at 0 °C under nitrogen, HOBt (103 mg, 0.750 mmol) and WSC (103 mg, 0.523 mmol) were added. After stirring for 30 min at 0 °C, the solution was added with **3a** (157 mg, 0.362 mmol) and DIPEA (165 mg, 1.28 mmol) and stirred for 2.5 h at room temperature. The solvent was evaporated and water was added (4 mL). The precipitate was filtered and dried. Purification by flash chromatography (CH_2Cl_2/MeOH 95:5) afforded the title compound as a yellow solid (yield 77%); mp 148 °C; R_f 0.36 (CH_2Cl_2/MeOH 95:5). ^{1}H NMR (DMSO-d_6) δ: 9.30 (s, 1H); 8.60 (d, J = 8.6 Hz, 1H); 8.25 (d, J = 8.6 Hz, 1H); 8.11 (brs, 1H); 7.98–7.85 (m, 1H); 7.85–7.70 (m, 1H); 7.39 (s, 1H); 6.80–6.60 (m, 2H); 6.50 (s, 1H); 5.48 (s, 2H); 5.39 (s, 2H); 4.38 (t, J = 6.9 Hz 2H); 4.03–3.97 (m, 1H); 3.70–3.50 (m, 2H); 3.25–3.10 (m, 2H); 198–1.80 (m, 2H); 1.38 (s, 18H); 0.87 (t, J = 7.0 Hz, 3H). ^{13}C NMR ($CDCl_3$) δ: 173.6, 171.0, 157.3, 156.9, 156.1, 152.0, 150.1, 149.3, 148.6, 145.7, 144.1, 130.8, 130.5, 128.4, 125.8, 125.1, 122.7, 118.8, 97.9, 73.9, 73.5, 72.7, 66.2, 55.8, 42.5, 38.9, 31.5, 28.2, 24.8, 7.7. HRMS(ESI$^+$): $[M + Na]^+$ calcd for $C_{36}H_{45}N_6O_{10}$ 721.3192; found 721.3163. Anal. calcd for $C_{36}H_{44}N_6O_{10}$: C, 59.99; H, 6.15; N, 11.66. Found: C, 59.76; H, 5.93; N, 11.81.

4.1.2. 2,3-d,l-Diamoniumtrifluoroacetate-N-[2′-(camptothecin-7-ylmethyleneaminooxy)-ethyl]-propionamide (**6a**)

TFA (2.75 mL) was dropped into a solution of **5a** (138 mg, 0.27 mmol) in CH_2Cl_2 (2.7 mL) at 0 °C. The resulting orange solution was stirred for 3 h at room temperature. The solvent was evaporated and Et_2O was added to obtain a precipitate. The solid was filtered and washed three times with Et_2O then dried to give the title compound as a yellow solid in quantitative yield; mp 120 °C. ^{1}H NMR (DMSO-d_6) δ: 9.35 (s, 1H); 8.90 (brs, 1H); 8.60 (d, J = 8.6 Hz, 1H); 8.50–8.00 (brm, 7H); 7.99–7.92 (m, 1H); 7.90–7.82 (m, 1H); 7.39 (s, 1H); 6.60 (brs, 1H); 5.50 (s, 2H); 5.35 (s, 2H); 4.44 (t, J = 7 Hz, 2H); 4.22–4.12 (m, 1H); 3.70–3.65 (m, 1H); 3.65–3.50 (m, 1H); 3.35–3.20 (m, 2H); 1.95–1.80 (m, 2H); 0.87 (t, J = 7.0 Hz, 3H). ^{13}C NMR (DMSO-d_6) δ: 172.8, 166.9, 166.0, 159.3, 158.8, 157.1, 152.8, 150.5, 149.0, 146.1, 145.5, 131.2, 130.9, 130.3, 128.8, 127.2, 125.3, 124.4, 119.7, 97.4, 97.0, 73.4, 72.8, 65.6, 65.2, 52.5, 50.6, 40.1, 30.7, 8.2. HRMS(ESI$^+$): $[M - 2CF_3COO^-]^+$ calcd for $C_{26}H_{30}N_6O_6$ 522.2221; found 522.2287. Anal. calcd for $C_{30}H_{30}F_6N_6O_{10}$: C, 48.13; H, 4.04; N, 11.23. Found: C, 47.90; H, 3.91; N, 10.85.

4.1.3. Dichloro{2,3-d,l-diamino-N-[2′-(camptothecin-7-ylmethyleneaminooxy)-ethyl]-propionamide}platinum (II) (**1a**)

A solution of K_2PtCl_4 (44 mg, 0.11 mmol) in water (0.40 mL) was prepared under a stream of nitrogen. The aqueous solution was added to a solution of compound **2a** (80 mg, 0.11 mmol) in water (2 mL) and the resulting mixture was stirred in the dark at room temperature under nitrogen for 3 h. The orange precipitate formed was filtered and washed twice with water, then with methanol and with Et_2O. After drying under vacuum the title compound was obtained as a yellow solid (yield 69%); mp 255 °C; R_f 0.30 (CH_2Cl_2/MeOH 7:1); ^{1}H NMR (DMSO-d_6) δ: 9.33 (s, 1H); 8.62 (d, J = 8.6 Hz, 1H); 8.50 (brs, 1H); 8.25 (d, J = 8.6 Hz, 1H); 8.00–7.79 (m, 1H); 7.85–7.75 (m, 1H); 7.40 (s, 1H); 6.58 (brs, 1H); 5.82 (brs, 1H); 5.49 (s, 2H); 5.40 (s, 2H); 5.11 (brs, 1H); 4.40 (t, J = 7.0 Hz, 2H); 3.70–3.50 (m, 3H); 3.40–3.30 (m, 2H), 1.95–1.80 (m, 2H); 0.87 (t, J = 7.0 Hz, 3H). ^{13}C NMR (DMSO-d_6) δ 172.9, 167.9, 167.0, 157.1, 152.9, 150.5, 149.1, 146.3, 145.6, 131.0, 130.3, 128.8, 127.4, 125.4, 124.7, 119.7, 97.2, 73.5, 72.8, 65.6, 61.7, 52.6, 40.7, 39.0, 30.6, 8.2. HRMS(ESI$^+$): $[M + Na]^+$ calcd for $C_{26}H_{28}Cl_2N_6NaO_6Pt$ 808.0987; found: 808.0958. Anal. calcd for $C_{26}H_{28}$ $Cl_2N_6O_6Pt$: C, 39.70; H, 3.59; Cl, 9.02; N, 10.69, Pt 24.80. Found: C, 39.82; H, 3.44; Cl, 9.35; N, 10.33; Pt 24.40.

4.1.4. [6-(1,3-Dioxo-1,3-dihydro-isoindol-2-yloxy)hexyl]carbamic acid tert-butyl ester (**7**)

To a solution of (6-hydroxyhexyl)carbamic acid tert-butyl ester [29] (730 mg, 3.36 mmol), triphenylphosphine (1.173 g, 4.48 mmol) and N-hydroxyphthalimide (731 mg, 4.48 mmol) in THF (45 mL) at 0 °C, diisopropyl azodicarboxylate (906 mg, 4.48 mmol) was dropped. After stirring overnight at room temperature, the solvent was evaporated and the residue was purified by flash chromatography (hexane/ethylacetate 3:7 then hexane/ethylacetate 2:8) and successively crystallized from MeOH to give the title compound as a white solid (yield 82%); mp 166 °C. R_f 0.34 (CH_2Cl_2/MeOH 95:5). ^{1}H NMR ($CDCl_3$) δ: 7.89–7.67 (m, 4H); 4.61 (brs, 1H); 4.15 (t, J = 6.7 Hz 2H); 3.18–3.00 (m, 2H); 1.41 (s, 9H); 1.85–1.20 (m, 8H). ^{13}C NMR ($CDCl_3$) δ 163.6, 156.0, 134.4 (×2), 128.9 (×2), 123.4 (×2), 78.3, 70.0, 40.4, 29.8, 28.4, 28.2, 28.0, 26.3, 25.2, 21.9. HRMS (ESI$^+$): $[M + Na]^+$ calcd for $C_{19}H_{26}N_2NaO_5$ 385.1734; found 385.1779. Anal. calcd for $C_{19}H_{26}N_2O_5$: C, 62.97; H, 7.23; N, 7.73. Found: C, 62.81; H, 7.02; N, 7.98.

4.1.5. O-(6-Aminohexyl)hydroxylamine dihydrochloride (**8**)

To a solution of compound **7** (1.260 g, 3.48 mmol) in MeOH (10.2 mL), hydrazine hydrate (0.522 g, 10.44 mmol) was added. The resulting mixture was refluxed for 1 h. The white solid was filtered, the solvent evaporated and the residue purified by flash chromatography (CH_2Cl_2: MeOH 99:1) to give (6-aminooxyhexyl)carbamic acid tert-butyl ester as a colorless oil in quantitative yield. R_f 0.25 (CH_2Cl_2/MeOH 95:5). ^{1}H NMR ($CDCl_3$) δ: 6.32 (brs, 1H); 4.01 (t, J = 6.6 Hz 2H); 3.15–3.02 (m, 2H); 1.44 (s, 9H), 1.89–1.20 (m, 8H). ^{13}C NMR ($CDCl_3$) δ: 156.1, 77.8, 75.2, 44.6, 29.8, 28.7 (×2), 28.6, 26.5, 25.7, 22.1. HRMS (ESI$^+$): $[M + Na]^+$ calcd for $C_{11}H_{25}N_2O_3$ 233.1860; found 233.1845.

To a solution of the above tert-butyl ester (389 mg, 1.67 mmol) in AcOEt (2.8 mL) at 0 °C, a 5.9 M solution of HCl in AcOEt was dropped. After 1 h at 0 °C the solvent was evaporated to obtain the title compound as a white solid (yield 97%); R_f 0.15 (CH_2Cl_2/MeOH 9:1). ^{1}H NMR (DMSO-d_6) δ: 10.90 (brs, 3H); 7.91 (brs, 3H); 3.97 (t, J = 6.7 Hz, 2H); 2.80–2.65 (m, 2H); 1.61–1.43 (m, 4H); 1.37–1.21 (m, 4H). ^{13}C NMR (DMSO-d_6) δ: 74.2, 27.3, 27.1, 25.7, 24.9 (one peak missing due to overlapping with solvent signal). The compound was used without further purification for the next step.

4.1.6. 7-(6-Aminohexyloxyiminomethyl)camptothecin (**3b**)

To a suspension of camptothecin-7-carbaldehyde (**4**) (150 mg, 0.39 mmol) in EtOH (3.8 mL) compound **8** (163 mg, 0.79 mmol) and pyridine (0.65 mL) were added. The resulting mixture was heated at reflux for 1 h, then the solvent was evaporated. The pure title compound was obtained as a yellow solid after crystallization from Et_2O/EtOH (yield 77%); mp 80 °C; R_f 0.20 (CH_2Cl_2/MeOH 90:10). ^{1}H NMR (DMSO-d_6) δ: 9.31 (s, 1H); 8.60 (d, J = 8.5 Hz, 1H); 8.20 (d, J = 8.5 Hz, 1H); 7.98–7.61 (m, 4H); 7.34 (s, 1H); 6.53 (brs, 1H); 5.42 (s, 2H); 5.29 (s, 2H); 4.34 (t, J = 6.7 Hz, 2H); 2.86–2.63 (m, 2H); 1.96–1.75 (m, 4H); 1.69–1.40 (m, 6H); 0.87 (t, J = 6.7 Hz, 3H). ^{13}C NMR (75 MHz, DMSO-d_6) δ 168.6, 166.8, 157.1, 152.9, 150.5, 149.1, 146.5, 145.6, 131.0, 130.3, 128.7, 127.4, 125.4, 124.7, 119.7, 97.2, 74.4, 72.8, 65.6, 52.6, 44.0, 31.3, 30.7, 28.2, 27.5, 26.8, 8.2. HRMS (ESI$^+$): $[M + H^+]$ calcd for $C_{27}H_{31}N_4O_5$ 491.2289; found 491.2266. Anal. calcd for $C_{27}H_{30}N_4O_5$: C, 66.11; H, 6.16; N, 11.42. Found: C. 66.32; H. 6.00; N. 11.63.

4.1.7. Dichloro{2,3-d,l-diamino-N-[2′-(camptothecin-7-ylmethyleneaminooxy)-hexyl]-propionamide}platinum (II) (**1b**)

To a solution of 7-(6-aminohexyloxyiminomethyl)CPT (70 mg, 0.14 mmol) and dichloro[(*d*,*l*)-diaminopropionic acid]platinum(II) [26] (106 mg, 0.29 mmol) in dry DMF (7 mL), EDC (137 mg, 0.71 mmol) and TEA (5 drops) were added under nitrogen. The resulting mixture was stirred at room temperature for 24 h in the

dark. The solvent was evaporated and water was added. The suspension was heated to 60 °C, and the yellow precipitate was filtered (yield 89%); mp 197 °C. R_f 0.37 (CH_2Cl_2/MeOH/TEA 90:10:0.1). ^{1}H NMR 600 MHz (DMSO-d_6) δ: 9.32 (s, 1H); 8.59 (d, J = 8.6 Hz, 1H); 8.20 (d, J = 8.6 Hz, 1H); 8.11 (brs, 1H), 7.95–7.80 (m, 1H); 7.80–7.72 (m, 1H); 7.34 (s, 1H); 6.52 (s, 1H); 5.79 (brs, 1H); 5.45–5.35 (m, 3H); 5.37 (s, 2H); 5.00 (brs, 1H); 4.33 (t, J = 7.0 Hz, 2H); 3.40–3.25 (m, 2H); 3.18–3.00 (m, 2H); 1.90–1.75 (m, 5H); 1.60–1.10 (m, 5H); 0.87 (s, 3H). ^{13}C NMR 150 MHz (DMSO-d_6) δ 187.2, 172.8, 166.5, 157.1, 152.9, 150.4, 149.1, 145.6, 145.2, 131.5, 130.9, 130.2, 128.7, 127.2, 125.4, 124.6, 119.6, 97.1, 75.3, 72.8, 65.6, 61.4, 52.6, 50.0, 30.7, 29.1, 29.0, 26.5, 25.4, 8.1. HRMS(ESI$^+$): $[M + Na]^+$ calcd for $C_{30}H_{36}Cl_2N_6NaO_6Pt$ 864.1613; found: 864.1601. Anal. calcd for $C_{30}H_{36}Cl_2N_6O_6Pt$: C, 42.76; H, 4.31; Cl, 8.41; N, 9.97; Pt, 23.15; found C, 42.91; H, 406; Cl, 8.25; N, 9.69; Pt, 23.30.

4.2. Molecular modeling

The five studied camptothecin derivatives were assembled and refined using a systematic conformer search followed by geometry optimization of the lowest energy structure with MOPAC (PM3 Method, RMS gradient 0.0100) [30]. The macromolecule (PDB deposition code: 1T8I) was prepared by removing the camptothecin molecule and adding polar hydrogen atoms, while the side chains of the disordered amino acid residues of the macromolecule complex were checked and rebuilt in DeepView [31]. The individual compounds were pre-positioned based on the coordinates of camptothecin from the X-ray structure.

The small molecule compounds and the macromolecule were further processed using the Autodock Tool Kit (ADT) [32]. Gasteiger–Marsili charges [33] were loaded on the small molecules in ADT and Cornell parameters used for the phosphorus atoms in the DNA. Solvation parameters were added to the final macromolecule structure using Addsol utility of Autodock. All docking runs were performed with Autodock 4 [34], using an empirical free energy function and Lamarckian Genetic Algorithm, with an initial population of 50 randomly placed individuals, a maximum number of 200 energy evaluations, a mutation rate of 0.02, a crossover rate of 0.80, and an elitism value of 1. For the local search, the so-called pseudo-Solis and Wets algorithm was applied using a maximum of 250 iterations per local search. The probability of performing local search on an individual in the population was 0.06, and the maximum number of consecutive failures before doubling or halving the local step size was 4. Fifty independent docking runs were carried out for each ligand. Results differing by less than 1.0 Å in positional root-mean-square deviation (rmsd) were clustered together and represented by the result with the most favorable free energy of binding. The grid maps representing the protein in the actual docking process were calculated with Autogrid. The grids (one for each atom type in the ligand, plus one for electrostatic interactions) were chosen to be sufficiently large to include the entire width of the DNA fragment in which the original inhibitor was posed, a portion of minor and major grooves, and the active site residues of Topoisomerase I. The dimensions of the grids were thus 80 × 80 × 50, with a spacing of 0.200 Å between the grid points and the center close to the cavity left by the ligand after its removal. The simpler intermolecular energy function based on the Weiner force field16 in Autodock was used to score the docking results.

4.2.1. Hybrid QM/MM calculations

In the current study, we used the pseudo-bond *ab-initio* QM/MM approach as implemented in Gaussian-03 [35]. For the QM/MM calculations, the DNA–Topoisomerase I-ligand system resulting from the docking study was first partitioned into a QM subsystem and an MM subsystem. The reaction system used a smaller QM subsystem consisting of the ligand and bases within 3.5 Å, whereas the rest of the system (the MM subsystem) was treated using the AMBER force field, together with a low memory convergence algorithm. The boundary problem between the QM and MM subsystems was treated using the pseudo-bond approach. With this QM/MM system, an iterative optimization procedure was applied to the QM/MM system, using BLYP/PW QM/MM calculations, leading to an optimized structure for the reactants. BLYP-STB and BP-STB calculations were carried out in order to check the dependence of the relative energies on the basis set and exchange correlation functional. The core electrons were frozen up to 4f for Pt, 2p for Cl and 1s for N. For Pt, scalar relativistic effects were taken into account. The convergence criterion used was set to obtain an energy gradient of $<10^{-4}$, using the twin-range cutoff method for non-bonded interactions, with a long-range cutoff of 14 Å and a short-range cutoff of 8 Å.

4.3. Assessment of cytotoxic activity on human cancer cell lines

The non-small cell lung cancer H460 cell line, the squamous carcinoma A431 cell line and the corresponding TPT-resistant A431/TPT and cisplatin-resistant A431/Pt sublines, the osteosarcoma U2OS cell line and the corresponding cDDP-resistant U2OS/Pt subline, the ovarian carcinoma IGROV-1 and A2780 cell lines and the corresponding Pt-resistant IGROV-1/Pt, IGROV-1/OHP and A2780/CP sublines were used. Cells were cultured in RPMI 1640 containing 10% FCS. Cytotoxicity was assessed by growth inhibition assay after a 1 h drug exposure. Compounds **1a**, **1b**, **6a** and **6b** were initially dissolved in dimetylsulphoxide and then diluted in sterile water. TPT and cDDP were dissolved and diluted in saline solution (0.9% sodium chloride). Twenty-four hours after seeding in well plates (from 30 × 10^3 to 120 × 10^3 cells/plate, depending on cell line), cells were exposed to the drugs and counted 72 h later by a Coulter Counter. Each experimental sample was run in triplicate. The IC_{50} was defined as the drug concentration causing 50% cell growth inhibition determined by dose response curves generated by testing at least 5 different drug concentrations. Combination studies were performed using cDDP concentrations producing 80–90% of cell growth.

4.4. Saccharomyces cerevisiae yeast strain and yeast spot test

JN2-134*top1-1 S. cerevisiae* strain (MATα rad52::LEU2, trp1, ade2-1, his7, ura3-52, ise1, top1, leu2), which lacks the endogenous TOP1 gene, was transformed with the empty vector (pEMBLyex4) or with the same vector containing the wild-type human DNA topoisomerase IB (pEZ-2hTop1) [36]. Yeast cells were maintained at 30 °C in synthetic complete medium lacking uracil (uracil-) and supplemented with 2% glucose. For the yeast spot test, cells were growth at 30 °C in uracil medium to an OD_{595} of 0.3. The yeast culture was then treated with camptothecins or cisplatin for 24 h. After treatment, aliquots of 10 μl were spotted onto plate uracil-. Following 3 days of incubation at 30 °C, images were acquired using the IMAGE MASTER VDS (Amersham Pharmacia Biotech).

4.5. Topoisomerase I-dependent DNA cleavage assay

A 3′-end labeled gel purified 751-bp BamHI–EcoRI fragment of SV40 DNA was used for the cleavage assay. SV40 plasmid was first linearized with BamHI enzyme and then 3′-labeled by using DNA polymerase I large (klenow) fragment (Invitrogen, Paisley, UK) in the presence of α^{32}P dGTP. The labeled DNA was then restricted with EcoRI enzyme, and the corresponding 751-bp was purified on agarose gel. Topoisomerase I DNA cleavage reactions (20,000 cpm/sample) were performed in 20 μl of 10 mM Tris–HCl (pH 7.6),

150 mM KCl, 5 mM $MgCl_2$, 0.1 mM dithiothreitol, and human recombinant enzyme (full length topoisomerase I) for 30 min at 37 °C [36]. Reactions were stopped by 0.5% SDS and 0.3 mg/ml of proteinase K for 45 min at 42 °C. Persistence of DNA cleavage at different time points was examined by adding 0.6 M NaCl after 30 min of incubation. After precipitation DNA was resuspended in denaturing buffer (80% formamide, 10 mM NaOH, 0.01 M EDTA and 1 mg/ml dyes) before loading on a denaturing 8% polyacrylamide gel in TBE buffer. Overall DNA cleavage levels were measured with a PhosphoImager 425 model (Molecular Dynamics).

4.6. Drug accumulation studies

Exponentially growing H460 cells (1×10^6) were seeded in 5 cm diameter dishes in triplicate and, 24 h later, they were exposed to equitoxic (IC_{50}) or equimolar (0.4 μM) concentrations of the drugs for 1 h. After treatment, cell monolayers were washed with ice-cold PBS, scraped, harvested and dissolved in 1 N NaOH. Total cellular Pt content was determined by flameless atomic absorption spectroscopy [37] (Model 3300, Perkin Elmer) or by inductively coupled plasma-mass spectrometry [38]. Cellular Pt levels were expressed as ng/10^6 cells, with cell number determined by counting parallel cultures. For each type of treatment at least three independent experiments were performed.

4.7. DNA platination studies

Exponentially growing H460 cells (3×10^6) were seeded in 5 cm diameter dishes in triplicate and, 24 h later, they were exposed to the drugs for 1 h at equitoxic (IC_{50}) or equimolar (0.4 μM) concentrations. DNA was then extracted according to standard procedures involving lysis in the presence of 1 mg/ml proteinase K overnight at 37 °C. DNA was then isolated following phenol extraction, ethanol precipitation, RNase treatment, and reprecipitation and finally was dissolved in 10 mM Tris–HCl (pH 7.4) and 1 mM EDTA. DNA content was determined spectrophotometrically and platinum content was measured by flameless atomic absorption spectroscopy (Model 3300, Perkin Elmer) or by inductively coupled plasma-mass spectrometry.

For the experiments with yeast cells, JN2-134*top1-1 S. cerevisiae* strain transformed with pEMBLyex4 or with pEZ-2hTop1 vectors was treated over night with 50 μM drug. Genomic DNA was obtained using MasterPure Yeast DNA purification kit (Epicentre biotechnologies, Wisconsin, USA) and the platinum content measured by inductively coupled plasma-mass spectrometry.

For cell free experiments, pCMV6neo vector (10 μg sample) was treated for 1 h at 37 °C with different compounds (50 μM) in the presence and absence of Topo I. After treatment, DNA was isolated following phenol extraction and ethanol precipitation. DNA concentration was determined spectrophotometrically, and platinum content was measured by flameless atomic absorption spectroscopy (Model 3300, Perkin Elmer).

4.8. DNA binding of camptothecins

EcoRV linearized pCMV6neo plasmid was used. Vector (200 ng sample) and CPT analogues (50 μM sample) were incubated in 20 μl of 10 mM Tris–HCl (pH 7.6), 150 mM KCl, 5 mM $MgCl_2$, 0.1 mM dithiothreitol for 1 h at 37 °C in the presence/absence of Topo I or BSA. After treatment, samples were loaded on 1% agarose gels or treated with 0.5% SDS and 0.3 mg/ml of proteinase K for 45 min at 42 °C (where indicated) and then loaded on 1% agarose gel. The DNA plasmid migration was determined after the ethidium bromide staining.

4.9. Antitumor activity

All experiments were carried out using female athymic Swiss nude mice, 7–10 weeks old (Charles River, Calco, Italy). Mice were maintained in laminar flow rooms keeping temperature and humidity constant. Mice had free access to food and water. Experiments were approved by the Ethics Committee for Animal Experimentation of the *Istituto Nazionale Tumori* of Milan according to institutional guidelines.

The compound was dissolved in DMSO/cremophor ELP. The solution was maintained at 4 °C. Before the treatment, the drug solution was suspended in cold saline (5 + 2.5 + 92.5 of final volume) under magnetic stirring. Drug was delivered in a volume of 10 ml/kg of body weight.

Cisplatinum Teva (clinical) was ready to use. Irinotecan was dissolved in sterile, distilled water keeping it under magnetic stirring for about 2 h.

Exponentially growing tumor cells (10^7 cells/mouse) were s.c. injected into the right flank of athymic nude mice. The tumor line was achieved by serial s.c. passages of fragments (about $2 \times 2 \times 6$ mm) from growing tumors into healthy mice as previously described [39]. Tumor fragments were implanted on day 0, and tumor growth was followed by biweekly measurements of tumor diameters with a Vernier caliper. Tumor volume (TV) was calculated according to the formula: $TV\ (mm^3) = d2 \times D/2$ where d and D are the shortest and the longest diameter, respectively. Drugs were delivered i.v. every fourth day for four times (q4dx4) starting when tumors were just palpable. The efficacy of the drug treatment was assessed as tumor volume inhibition percentage (TVI%) in treated versus control mice, calculated as: TVI% = 100 − (mean TV treated/mean TV control × 100). The toxicity of the drug treatment was determined as body weight loss and lethal toxicity. Deaths occurring in treated mice before the death of the first control mouse were ascribed to toxic effects.

4.10. Statistical analysis

Two-tailed Student's *t* test was used for statistical comparison of drug uptake and DNA platination data as well as of tumor volumes in mice.

Acknowledgments

We are indebted to MIUR (PRIN 2009 project) and to the *Associazione Italiana per la Ricerca sul Cancro*, Milan, for financial support. We thank Ms. Betty Johnston for editorial assistance.

Appendix A. Supplementary data

Supplementary data related to this article can be found at http://dx.doi.org/10.1016/j.ejmech.2013.02.022.

References

[1] B. Rosenberg, L. Van Camp, J.E. Trosko, V. Mansour, Platinum compounds: a new class of potent antitumour agents, Nature 222 (1969) 385–386.
[2] a) L.R. Kendall, N.P. Farrell, Platinum-based Drugs in Cancer Therapy, Humana Press, Totowa, NJ, 2000;
b) U. Olszewski, G. Hamilton, A better platinum-based anticancer drug yet to come? Anti-Cancer Agents Med. Chem. 10 (2010) 293–301;
c) J. Zhang, L. Wang, Z. Xing, D. Liu, J. Sun, X. Li, Y. Zhang, Status of bi- and multi-nuclear platinum anticancer drug development, Anti-Cancer Agents Med. Chem. 10 (2010) 272–282.
[3] R.T. Skeel, Antineoplastic drugs and biologic response modifiers: classification, use and toxicity of clinically useful agents, in: R.T. Skeel (Ed.), Handbook of Cancer Chemotherapy, seventh ed., Lippincott Williams and Wilkins, 1999, pp. 63–143.

[4] a) P.A. Andrews, S.B. Howell, Cellular pharmacology of cisplatin: perspectives on mechanisms of acquired resistance, Cancer Cells 2 (1990) 35–43;
b) M.M.K. Shahzad, G. Lopez-Berestein, A.K. Sood, Novel strategies for reversing platinum resistance, Drug Resist. Updates 12 (2009) 148–152;
c) J.J. Ju, Unlocking the molecular mechanisms of DNA repair and platinum drug resistance in cancer chemotherapy, Curr. Drug Ther. 4 (2009) 19–28.

[5] a) K.R. Harrap, Initiatives with platinum- and quinazoline-based antitumor molecules-Fourteenth Bruce F. Cain memorial award lecture, Cancer Res. 55 (1995) 2761–2768;
b) A.V. Klein, T.W. Hambley, Platinum drug distribution in cancer cells and tumors, Chem. Rev. 109 (2009) 4911–4920.

[6] a) H. Niedner, R. Christen, X. Lin, A. Kondo, S.B. Howell, Identification of genes that mediate sensitivity to cisplatin, Mol. Pharmacol. 60 (2001) 1153–1160;
b) Y. Nieto, DNA-binding agents, Cancer Chemother. Biol. Response Modif. 22 (2005) 163–203;
c) R. Guddneppanavar, U. Bierbach, Adenine-N3 in the DNA minor groove–an emerging target for platinum containing anticancer pharmacophores, Anti-Cancer Agents Med. Chem. 7 (2007) 125–138;
d) R.P. Feazell, N. Nakayama-Ratchfor, H. Dai, S.J. Lippard, Soluble single-walled carbon nanotubes as longboat delivery systems for platinum(IV) anticancer drug design, J. Am. Chem. Soc. 129 (2007) 8438–8439.

[7] F. Zunino, G. Pratesi, F. Formelli, A. Pasini, Evaluation of a platinum–doxorubicin complex in experimental tumor systems, Invest. New Drugs 8 (1990) 341–345.

[8] a) M.D. Temple, W.D. McFadyen, R.J. Holmes, W.A. Denny, V. Murray, Interaction of cisplatin and DNA-targeted 9-aminoacridine platinum complexes with DNA, Biochemistry 39 (2000) 5593–5599;
b) M.D. Temple, P. Recabarren, W.D. McFadyen, R.J. Holmes, W.A. Denny, V. Murray, The interaction of DNA-targeted 9-aminoacridine-4-carboxamide platinum complexes with DNA in intact human cells, Biochim. Biophys. Acta 1574 (2002) 223–230.

[9] a) B.B. Hasinoff, X. Wu, Y. Yang, Synthesis and characterization of the biological activity of the cisplatin analogs, *cis*-$PtCl_2$(dexrazoxane) and *cis*-$PtCl_2$(levrazoxane), of the topoisomerase II inhibitors dexrazoxane (ICRF-187) and levrazoxane (ICRF-186), J. Inorg. Biochem. 98 (2004) 616–624;
b) M.S. Robillard, A. Valentijn, P.M. Rob, N.J. Meeuwenoord, G.A. Van der Marel, J.H. Van Boom, J. Reedijk, The first solid-phase synthesis of a peptide-tethered platinum(II) complex, Angew. Chem. Int. Ed. 39 (2000) 3096–3099.

[10] a) R.A. Alderden, H.R. Mellor, S. Modok, T.W. Hambley, R. Callaghan, Cytotoxic efficacy of an anthraquinone linked platinum anticancer drug, Biochem. Pharmacol. 71 (2006) 1136–1145;
b) D. Gibson, I. Binyamin, M. Haj, I. Ringel, A. Ramu, J. Katzhendler, Anthraquinone intercalators as carrier molecules for second-generation platinum anticancer drugs, Eur. J. Med. Chem. 32 (1997) 823–831.

[11] S. D'Errico, G. Oliviero, V. Piccialli, J. Amato, N. Borbone, V. D'Atri, F. D'Alessio, R. Di Noto, F. Ruffo, F. Salvatore, G. Piccialli, Solid-phase synthesis and pharmacological evaluation of novel nucleoside-tethered dinuclear platinum(II) complexes, Bioorg. Med. Chem. Lett. 21 (2011) 5835–5838.

[12] W. Du, Towards new anticancer drugs: a decade of advances in synthesis of camptothecins and related alkaloids, Tetrahedron 59 (2003) 8649–8687.

[13] V.J. Venditto, E.E. Simanek, Cancer therapies utilizing the camptothecins: a review of the in vivo literature, Mol. Pharma. 7 (2010) 307–349.

[14] Y.H. Hsiang, R. Hertzberg, S.M. Hecht, L.F. Liu, Camptothecin induces protein-linked DNA breaks via mammalian DNA topoisomerase I, J. Biol. Chem. 260 (1985) 14873–14878.

[15] L.F. Liu, S.D. Desai, T.K. Li, Y. Mao, M. Sun, S.P. Sim, Mechanism of action of camptothecin, Ann. N. Y. Acad. Sci. 922 (2000) 1–10.

[16] Y. Pommier, Topoisomerase I inhibitors: camptothecins and beyond, Nat. Rev. Cancer 6 (2006) 789–802.

[17] a) E. Andreopoulou, T. Chen, L. Liebes, J. Curtin, S. Blank, R. Wallach, H. Hochster, F. Muggia, Phase 1/pharmacology study of intraperitoneal topotecan alone and with cisplatin: potential for consolidation in ovarian cancer, Cancer Chemother. Pharmacol. 68 (2011) 457–463;
b) J.P. van Meerbeeck, D.A. Fennell, D.K. De Ruysscher, Small-cell lung cancer, Lancet 378 (2011) 1741–1755;
c) A. Stein, D. Arnold, Oxaliplatin: a review of approved uses, Exp. Opin. Pharmacother. 13 (2012) 125–137.

[18] a) S. Dallavalle, L. Merlini, G. Morini, L. Musso, S. Penco, G.L. Beretta, S. Tinelli, F. Zunino, Synthesis and cytotoxic activity of substituted 7-aryliminomethyl derivatives of camptothecin, Eur. J. Med. Chem. (2004) 507–513;
b) S. Dallavalle, A. Ferrari, L. Merlini, S. Penco, N. Carenini, P. Perego, M. De Cesare, G. Pratesi, F. Zunino, Novel cytotoxic 7-iminomethyl and 7-aminomethyl derivatives of camptothecin, Bioorg. Med. Chem. Lett. 11 (2001) 291–294.

[19] S. Dallavalle, A. Ferrari, B. Biasotti, L. Merlini, S. Penco, G. Gallo, M. Marzi, M.O. Tinti, R. Martinelli, C. Pisano, P. Carminati, N. Carenini, G. Beretta, P. Perego, M. De Cesare, G. Pratesi, F. Zunino, Novel 7-oxyiminomethyl derivatives of camptothecin with potent in vitro and in vivo antitumor activity, J. Med. Chem. 44 (2001) 3264–3274.

[20] S. Dallavalle, G. Giannini, D. Alloatti, A. Casati, E. Marastoni, L. Musso, L. Merlini, G. Morini, S. Penco, C. Pisano, S. Tinelli, M. De Cesare, G.L. Beretta, F. Zunino, Synthesis and cytotoxic activity of polyamine analogues of camptothecin, J. Med. Chem. 49 (2006) 5177–5186.

[21] a) C. Pisano, M. De Cesare, G.L. Beretta, V. Zuco, G. Pratesi, S. Penco, L. Vesci, R. Foderà, F.F. Ferrara, P. Carminati, S. Dallavalle, G. Morini, L. Merlini, A. Orlandi, F. Zunino, Preclinical profile of antitumor activity of a novel hydrophilic camptothecin, ST1968, Mol. Cancer Ther. 7 (2008) 2051–2059;
b) M. De Cesare, G.L. Beretta, S. Tinelli, V. Benedetti, G. Pratesi, S. Penco, S. Dallavalle, L. Merlini, C. Pisano, P. Carminati, F. Zunino, Preclinical efficacy of ST1976, a novel camptothecin analog of the 7-oxyiminomethyl series, Biochem. Pharmacol. 73 (2007) 656–664;
c) G.L. Beretta, V. Zuco, M. De Cesare, P. Perego, N. Zaffaroni, Namitecan: a hydrophilic camptothecin with a promising preclinical profile, Curr. Med. Chem. 19 (2012) 3488–3501.

[22] a) A.X. Zhu, N. Ready, J.W. Clark, H. Safran, A. Amato, N. Salem, S. Pace, X. He, N. Zvereva, T.J. Lynch, D.P. Ryan, J.G. Supko, Phase I and pharmacokinetic study of gimatecan given orally once a week for 3 of 4 weeks in patients with advanced solid tumors, Clin. Cancer Res. 15 (2009) 374–381;
b) S. Pecorelli, I. Ray-Coquard, O. Tredan, N. Colombo, G. Parma, G. Tisi, D. Katsaròs, C. Lhommé, A.A. Lissoni, J.B. Vermorken, A. du Bois, A. Poveda, L. Frigerio, P. Barbieri, P. Carminati, S. Brienza, J.P. Guastalla, Phase II of oral gimatecan in patients with recurrent epithelial ovarian, fallopian tube or peritoneal cancer, previously treated with platinum and taxanes, Ann. Oncol. 21 (2010) 759–765.

[23] S. Dallavalle, D. Granza Rocchetta, L. Musso, L. Merlini, G. Morini, S. Penco, S. Tinelli, G.L. Beretta, F. Zunino, Synthesis and cytotoxic activity of new 9-substituted camptothecins, Bioorg. Med. Chem. Lett. 18 (2008) 2781–2787.

[24] B.L. Stayer, M.D. Feese, M. Cushman, Y. Pommier, D. Zembower, L. Stewart, A.B. Burgin, Structures of three classes of anticancer agents bound to the human topoisomerase I–DNA covalent complex, J. Med. Chem. 48 (2005) 2336–2345.

[25] S. Moradell, J. Lorenzo, A. Rovira, Water-soluble platinum(II) complexes of diamine chelating ligands bearing amino-acid type substituents: the effect of the linked amino acid and the diamine chelate ring size on antitumor activity, and interactions with 50-GMP and DNA, J. Inorg. Biochem. 98 (2004) 1933–1946.

[26] J. Altman, M. Wilchek, Platinum (II) complexes with diaminopropionic acid as oxygen-bound unidentate, nitrogen–oxygen and nitrogen–nitrogen chelate complexes, Inorg. Chim. Acta 101 (1985) 171–173.

[27] a) J. Ma, M. Maliepaard, K. Nooter, A.W. Boersma, J. Verweij, G. Stoter, J.H. Schellens, Synergistic cytotoxicity of cisplatin and topotecan or SN-38 in a panel of eight solid-tumor cell lines in vitro, Cancer Chemother. Pharmacol. 41 (1998) 307–316;
b) F. Goldwasser, L. Bozec, N. Zeghari-Squalli, J.L. Misset, Cellular pharmacology of the combination of oxaliplatin with topotecan in the IGROV-1 human ovarian cancer cell line, Anticancer Drugs 10 (1999) 195–201;
c) F. Goldwasser, M. Valenti, R. Torres, K.W. Kohn, Y. Pommier, Potentiation of cisplatin cytotoxicity by 9-aminocamptothecin, Clin. Cancer Res. 2 (1996) 687–693;
d) J.P. Lima, L.V. dos Santos, E.C. Sasse, C.S. Lima, A.D. Sasse, Camptothecins compared with etoposide in combination with platinum analog in extensive stage small cell lung cancer: systematic review with meta-analysis, J. Thorac. Oncol. 12 (2010) 1986–1993.

[28] a) K. Aoe, K. Kiura, H. Ueoka, M. Tabata, M. Chikamori, H. Kohara, M. Harada, M. Tanimoto, Cisplatin down-regulates topoisomerase I activity in lung cancer cell lines, Anticancer Res. 24 (2004) 3893–3897;
b) J. Malina, O. Vrana, V. Brabec, Mechanistic studies of the modulation of cleavage activity of topoisomerase I by DNA adducts of mono- and bifunctional Pt-II complexes, Nucleic Acids Res. 37 (2009) 5432–5442.

[29] D.E. Bergbreiter, P.L. Osburn, C. Li, Soluble polymer-supported catalysts containing azo dyes, Org. Lett. 4 (2002) 737–740.

[30] J.J.P. Stewart, Optimization of parameters for semiempirical methods V: modification of NDDO approximations and application to 70 elements, J. Mol. Model. 13 (2007) 1173–1213.

[31] http://spdbv.vital-it.ch/content.html.

[32] M. Sanner, F. Python, A programming language for software integration and development, J. Mol. Graphics Model. 17 (1999) 57–61.

[33] J. Gasteiger, M. Marsili, Iterative partial equation of orbital electronegativity–a rapid access to atomic charges, Tetrahedron 36 (1980) 3219–3228.

[34] a) G.M. Morris, D.S. Goodsell, R.S. Halliday, R. Huey, W.E. Hart, R.K. Belew, A.J. Olson, Automated docking using a Lamarckian genetic algorithm and an empirical binding free energy function, J. Comput. Chem. 19 (1998) 1639–1662;
b) R. Huey, G.M. Morris, A.J. Olson, D.S. Goodsell, A semiempirical free energy force field with charge-based desolvation, J. Comput. Chem. 28 (2007) 1145–1152.

[35] G.W.T.M.J. Frisch, H.B. Schlegel, G.E. Scuseria, M.A. Robb, J.R. Cheeseman, J.A. Montgomery, T. Vreven, K.N. Kudin, J.C. Burant, J.M. Millam, S.S. Iyengar, J. ;Tomasi, V. Barone, B. Mennucci, M. Cossi, G. Scalmani, N. Rega, G.A. Petersson, H. Nakatsuji, M. Hada, M. Ehara, K. Toyota, R. Fukuda, J. Hasegawa, M. Ishida, T. Nakajima, Y. Honda, O. Kitao, H. Nakai, M. Klene, X. Li, J.E. Knox, H.P. Hratchian, J.B. Cross, V. Bakken, C. Adamo, J. Jaramillo, R. Gomperts, R.E. Stratmann, O. Yazyev, A.J. Austin, R. Cammi, C. Pomelli, J.W. Ochterski, P.Y. Ayala, K. Morokuma, G.A. Voth, P. Salvador, J.J. Dannenberg, V.G. Zakrzewski, S. Dapprich, A.D. Daniels, M.C. Strain,

O. Farkas, D.K. Malick, A.D. Rabuck, K. Raghavachari, J.B. Foresman, J.V. Ortiz, Q. Cui, A.G. Baboul, S. Clifford, J. Cioslowski, B.B. Stefanov, G. Liu, A. Liashenko, P. Piskorz, I. Komaromi, R.L. Martin, D.J. Fox, T. Keith, M.A. Al-Laham, C.Y. Peng, A. Nanayakkara, M. Challacombe, P.M.W. Gill, B. Johnson, W. Chen, M.W. Wong, C. Gonzalez, J.A. Pople, Gaussian 03, Revision C.02, Gaussian, Inc., Wallingford CT, 2004.

[36] G.L. Beretta, M. Binaschi, E. Zagni, L. Capuani, G. Capranico, Tethering a type IB topoisomerase to a DNA site by enzyme fusion to a heterologous site-selective DNA-binding protein domain, Cancer Res. 59 (1999) 3689–3697.

[37] G.L. Beretta, L. Gatti, S. Tinelli, E. Corna, D. Colangelo, F. Zunino, P. Perego, Cellular pharmacology of cisplatin in relation to the expression of human copper transporter CTR1 in different pairs of cisplatin-sensitive and -resistant cells, Biochem. Pharmacol. 68 (2004) 283–291.

[38] E. Gabano, D. Colangelo, A.R. Ghezzi, D. Osella, The influence of temperature on antiproliferative effects, cellular uptake and DNA platination of the clinically employed Pt(II)-drugs, J. Inorg. Biochem. 102 (2008) 629–635.

[39] G. Pratesi, C. Manzotti, M. Tortoreto, E. Prosperi, F. Zunino, Effects of 5-FU and cis-DDP combination on human colorectal tumor xenografts, Tumori 75 (1989) 60–65.